

7-29-2011

# Design of a Retractable Vane for a Vertical Axis Wind Turbine

Thomas Powers

*Olivet Nazarene University*, [tpowers1@olivet.edu](mailto:tpowers1@olivet.edu)

Follow this and additional works at: [https://digitalcommons.olivet.edu/engn\\_stsc](https://digitalcommons.olivet.edu/engn_stsc)



Part of the [Energy Systems Commons](#)

---

## Recommended Citation

Powers, Thomas, "Design of a Retractable Vane for a Vertical Axis Wind Turbine" (2011). *Student Scholarship – Engineering*. 1.  
[https://digitalcommons.olivet.edu/engn\\_stsc/1](https://digitalcommons.olivet.edu/engn_stsc/1)

This Article is brought to you for free and open access by the Engineering at Digital Commons @ Olivet. It has been accepted for inclusion in Student Scholarship – Engineering by an authorized administrator of Digital Commons @ Olivet. For more information, please contact [digitalcommons@olivet.edu](mailto:digitalcommons@olivet.edu).

OLIVET NAZARENE UNIVERSITY

# Design of a Retractable Vane for a Vertical Axis Wind Turbine

---

A Pence Boyce Research Project

**Thomas C. Powers**  
**tpowers1@live.olivet.edu**

**Faculty Mentor:**  
**Dr. Joseph B. Schroeder**  
**Schroed@olivet.edu**

**7/29/2011**

## Abstract

This study investigated the impact of vane design for a retractable vane Savonius style Vertical Axis Wind Turbine (VAWT). Five designs were tested in a wind tunnel to find which design produces the most torque on the rotor, and to obtain a value for drag coefficient and lift coefficient. Eight position angles were selected to represent the infinite number of vane positions possible compared to the direction of the wind. The wind tunnel was not able to generate air speeds great enough to reach the Reynolds numbers ( $Re$ ) required for similarity. Reynolds number independence was sought to justify extrapolation to the required  $Re$ . In many cases extrapolation was not reasonable. Instead the data was analyzed assuming a “best approximation” range for each vane and position. The testing setup introduced extra uncertainty that was considered in analysis, and presumed to be harmonic motion of the setup and/or the evidence of vortex shedding. The best vane design proved to be an airfoil with a curved trailing edge, although all designs proved feasible for power production. The curved airfoil design reduced possible vortex shedding and the induced drag to become the most consistent, high torque producer of the five designs. The net torque seemed to be influenced more by the vane position than the vane design. Thus, more importance may lie in the design of the retraction mechanism than in the vane design. With this curved airfoil design, research can extend to a study of retraction mechanisms, power production systems, and, eventually, construction.

## Table of Contents

Abstract.....	2
List of Figures.....	4
List of Tables .....	4
Introduction.....	5
Background.....	5
Historical Background.....	5
Analytical Background .....	7
Scope .....	9
Setup and Procedures .....	9
Data Results and Calculations.....	13
Analysis and Discussion.....	19
Conclusion .....	21
Relation to the Ultimate Goal .....	22
Cost Report .....	22
Research Impact.....	23
Special Thanks .....	23
References.....	24
Appendix .....	25
Wind Tunnel Setup (Drag).....	25
Configuring LoggerPro.....	25
Wind Tunnel Setup (Lift).....	26
Testing Procedure.....	27

## List of Figures

Figure 1: Concept for ultimate goal.....	5
Figure 2: Horizontal Axis Turbines [8]. ....	6
Figure 3: Vertical Axis Wind Turbines [8].....	7
Figure 4: Reynolds number independence [9]. ....	8
Figure 5: Vane Designs .....	10
Figure 6: The eight selected vane positions on the rotor. ....	11
Figure 7: The Flotek 360 that was used for the testing.....	12
Figure 8: Drag Setup .....	12
Figure 9: Lift Setup .....	12
Figure 10: The graph of drag coefficient vs. Reynolds number of the Curved Airfoil. ....	14
Figure 11: The graph of lift coefficient vs. Reynolds number of the Curved Airfoil.....	14
Figure 12: The graph of drag coefficient vs. the Reynolds number of the Rectangular Airfoil.....	15
Figure 13: The graph of lift coefficient vs. Reynolds number of the Rectangular Airfoil.....	15
Figure 14: The graph of drag coefficient vs. Reynolds number of the Regular Vane. ....	16
Figure 15: The graph of lift coefficient vs. Reynolds number of the Regular Vane. ....	16
Figure 16: The graph of drag coefficient vs. Reynolds number of the Regular Vane with Lip.....	17
Figure 17: The graph of lift coefficient vs. Reynolds number of the Regular Vane with Lip. ....	17
Figure 18: The graph of drag coefficient vs. Reynolds number of the Airfoil with Lip.....	18
Figure 19: The graph of lift coefficient vs. Reynolds number of the Airfoil with Lip.....	18
Figure 20: Data fitting the Reynolds number independence curve. ....	20
Figure 21: Vane comparison.....	21
Figure 22: Low Friction Track used for the Drag Tests. ....	25
Figure 23: Force Sensor location for Drag tests.....	25
Figure 24: Setup for Sensor calibration. ....	26
Figure 25: Force Sensor location for Lift tests.....	27

## List of Tables

Table 1: The Coefficients of Drag and Lift obtained from the graphs.....	19
Table 2: Estimated Values for Torque.....	19
Table 3: Cost Report.....	22

## Introduction

In the global search for alternate ways to harness energy, wind has been one of the first sources investigated. All over the United States, Horizontal Axis Wind Turbines (HAWT) have been erected to harvest the power of the wind. Comparatively little research has been done with Vertical Axis Wind Turbines (VAWT) compared to the HAWT due to the typically low power conversion efficiency [1]. One benefit of the VAWT is that it does not need to be moved or changed to face the wind correctly. The VAWT will function regardless of the wind direction. The efficiency of the turbine will be affected by the way the vanes capture the wind directed at it, and also by how well the vanes escape the wind when moving into it. Therefore, this study seeks to design a functional vane shape which allows for retraction, and to design a retraction mechanism to position the vane relative to the wind to maximize efficiency. The ultimate goal of this project is to construct a vertical axis wind turbine that has retractable vanes (Figure 1) with inexpensive, readily available materials and locate it on Olivet Nazarene University's campus. The proposed scale is to be sized for an individual building; one meter diameter rotor.

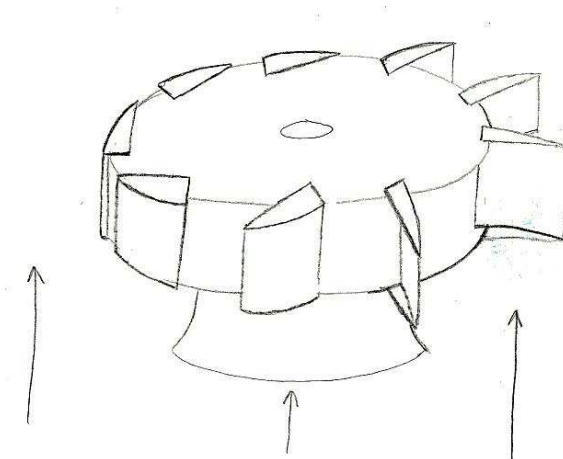


**Figure 1: Concept for ultimate goal.**

## Background

### Historical Background

Using wind power for electricity generation was first done in Denmark in the late 1800s, but did not catch on in the United States until the 1930s [2]. At this time the US Rural Electrification Administration started programs that used the U.S. multi-bladed farm windmill (Figure 2) to bring electric power to the west and the plains of the United States [3]. Enthusiasm for wind technology peaked during World War II. After the war the enthusiasm for wind power declined until the energy crisis that started in the 1970s. During this time the primary investigated use for wind power was the recharging of batteries. Beginning in the '70s the focus turned to mass power production, especially in Europe and North America. Many of the first wind turbines were not successful. With the government funding needed for a good kick start, the US imported many wind turbines from countries such as Denmark and Germany.

Even though the US investigated wind power early on, many nations in Europe have always been one step ahead of the other countries with installing quality machines. [2]

The type of wind turbine that has become popular has been the propeller type turbines that are classified as Horizontal Axis Wind Turbines (Figure 2). These are the turbines that are seen in the huge wind farms that stretch for miles on the Midwest plains and in Wyoming. These three bladed turbines have also been located near the coasts, where they are even larger than the ones found at a typical wind farm inland [3]. The VAWT rotates around a vertical axis, moving parallel to the ground rather than perpendicular to it as the HAWT do. The VAWT (Figure 3) have not been as popular due to the lower efficiencies that are involved with them [1]. The most efficient type of VAWT is the Darrieus turbine, which uses airfoils to create lift that maintains rotation. The main difficulty of this design is that it is not self-starting. The other main VAWT is called the Savonius turbine, and a basic set up is easily fabricated by cutting an oil barrel in half and connecting the two parts to a shaft. Though the VAWT have not received near the attention of their horizontal counterparts, there still has been some research done, much of it to improve the efficiency especially of the Savonius rotor [4] [5] [6] [7]. Some of these include shields and funnels that direct the air to the side that allows for wind capture. This added feature alone has increased the efficiency by 10 % [7]. The Savonius design is the least efficient rotor type, but it is this design that this research's design resembles most closely. The largest difference in this study's design is the retracting capability of the vanes, which will decrease drag and improve the efficiency. [2] [8] [5] [6] [7]

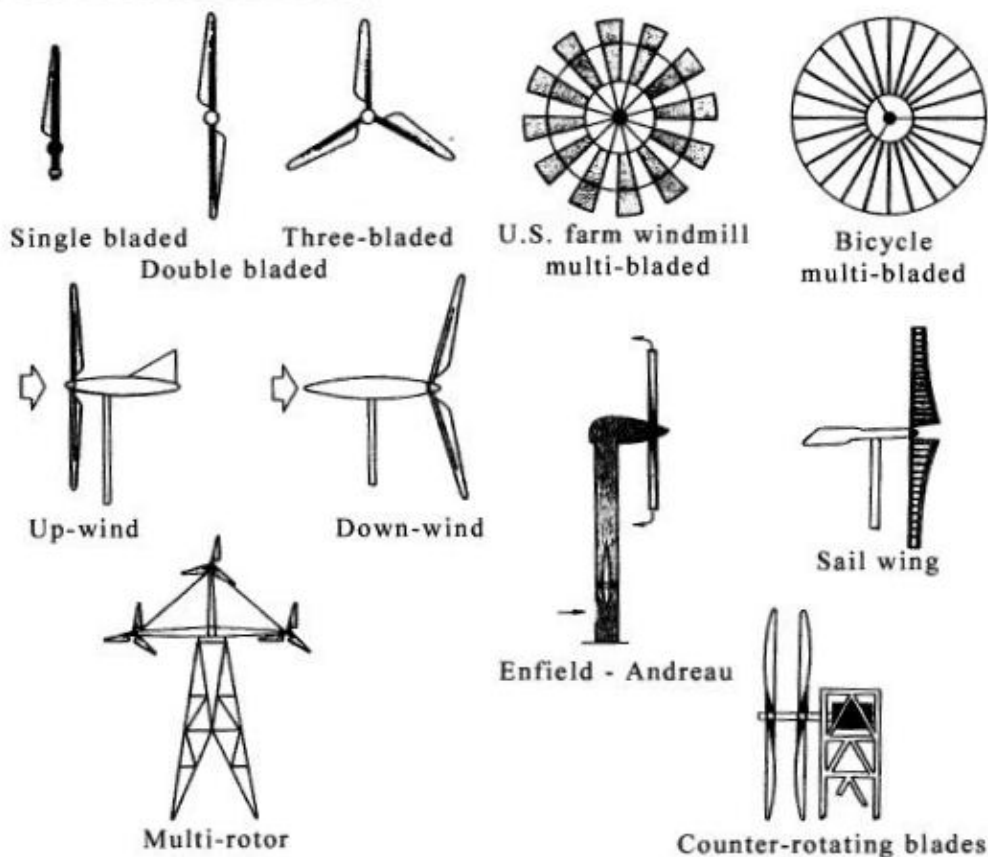


**Figure 2: Horizontal Axis Turbines [8].**

### Analytical Background

In order to create a VAWT that will function as desired, various areas must be investigated. These areas include the vane shape, retraction mechanism, friction of moving parts, generator capabilities, and power analysis. In this research the vane shape is primarily investigated. Wind tunnels are often used to test and compare various wind turbine designs. When using a wind tunnel, the principles of dimensional analysis and similarity are required to compare different design ideas correctly.

The principle of similarity consists of three parts: geometric, kinematic, and dynamic similarity. According to the geometric similarity condition, the model must be the exact same shape, although it may be scaled by a consistent factor. Kinematic similarity entails that the velocity at any given point on the model is proportional to the velocity at that same point on the prototype. Dynamic similarity describes proportional forces at any given point on the model and prototype. [9]

Non-dimensional numbers are typically used to ensure similarity because the units do not interfere with the calculations. The most famous non-dimensional number is called the Reynolds number. It consists of the viscous force divided out of the inertial force. It can be expressed as

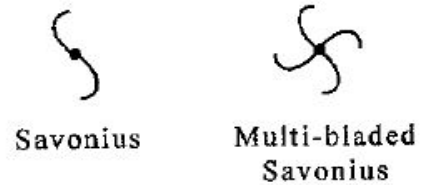
—

**Equation 1**

Where

- $\rho$  is the density of the fluid
- $V$  is the speed of the fluid passing over the object
- $L$  is the characteristic length of the object
- $\mu$  is the viscosity of the fluid [9]

#### Primarily drag-type



#### Primarily lift-type

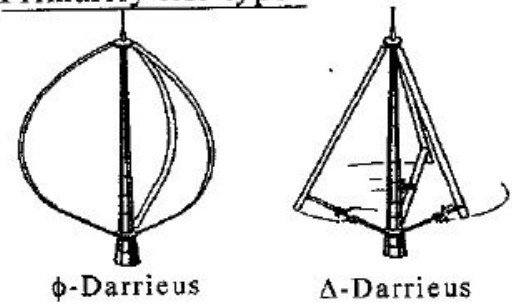


**Figure 3: Vertical Axis Wind Turbines [8].**



Two other non-dimensional parameters that are discussed when looking at vane shape are the coefficients of drag and lift. These are expressed as

$$\text{Equation 2}$$

Where

- $F_D$  is the Drag Force
- $F_L$  is the Lift Force
- $\rho$  is the density of the air
- $V$  is the speed of the air passing over the object
- $A$  is the frontal area (if not airfoil)
- $A$  is planform area (if airfoil) [9]

These numbers can be used to identify similarity. The Reynolds number for the prototype should match the Reynolds number for the model. If the Reynolds number cannot be matched because of the physical limitations of the wind tunnel, such as max speed, size, etc. several things can be done. It is possible to use a bigger wind tunnel and model, use a different fluid, change the pressure, or as a last resort, extrapolate the results to the required Reynolds number. This last option is possible due to Reynolds number independence. As the Reynolds number increases, the coefficient of drag gradually becomes independent of the Reynolds number (see Figure 4). [9]

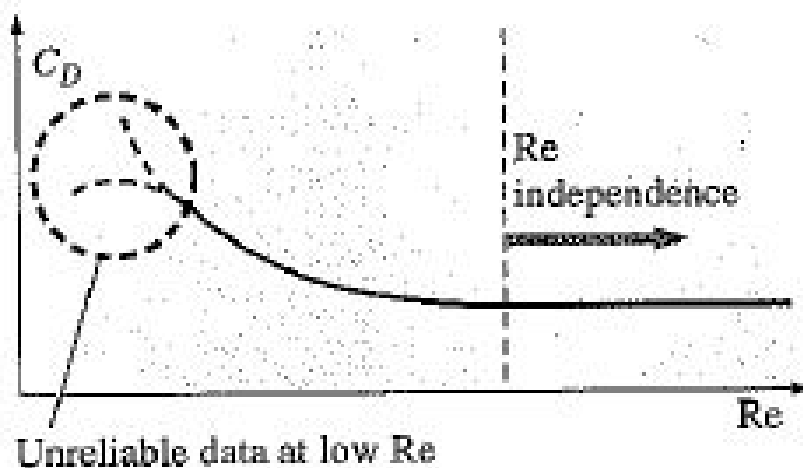


**Figure 4: Reynolds number independence [9].**

The wind tunnel velocities are obtained using a manometer, which uses Bernoulli's equation to relate the pressure and velocity differences inside the wind tunnel test section and outside the wind tunnel. When the pressure difference is known, the airspeed is calculated using Equation 3.

$$V = \sqrt{\frac{2\Delta P}{\rho}} \quad \text{Equation 3}$$

Where

- V is the airspeed
- $\Delta P$  is the pressure given with the manometer
- $\rho$  is the air density [9]

With the information gathered by the wind tunnel experiments in terms of drag and lift coefficients, the forces present on the rotor assembly can be estimated and used to predict the net torque on the rotor. The greater the torque is, the more power that may be harvested from the turbine.

## Scope

This study compares five vane designs using the coefficients of drag and lift. Three of the designs were developed using the basics of Aerodynamics discussed in [9], [10], and [11]. The goal of this study is to identify which of these five vanes can generate the largest net torque on the rotor.

This study focuses on the:

- Vane Design
- Coefficients of Drag and Lift
- Drag and Lift Forces
- Reynolds numbers
- Individual vane Torque
- Net Torque
- Airfoil Retracting Mechanism

This study does not investigate

- Power
- Generators
- Circuitry
- Construction of Prototype
- Other Retraction Mechanisms

## Setup and Procedures

First the five vane designs were developed. The following designs were chosen: the (a) bucket vane, (b) curved airfoil vane, (c) straight airfoil vane, (d) bucket vane with a lip, and (e) straight airfoil

vane with a lip (Figure 5). When researching retraction mechanisms, the idea of extending airfoils to retract the vane using its lift and drag components came forth. After researching airfoils and estimating the lift and drag forces required to act as a closing mechanism, the airfoil design resembling the NACA2712 type airfoil was chosen [12] and drag components came forth. After researching airfoils and estimating the lift and drag forces required to act as a closing mechanism, the airfoil design resembling the NACA2712 type airfoil was chosen [12]

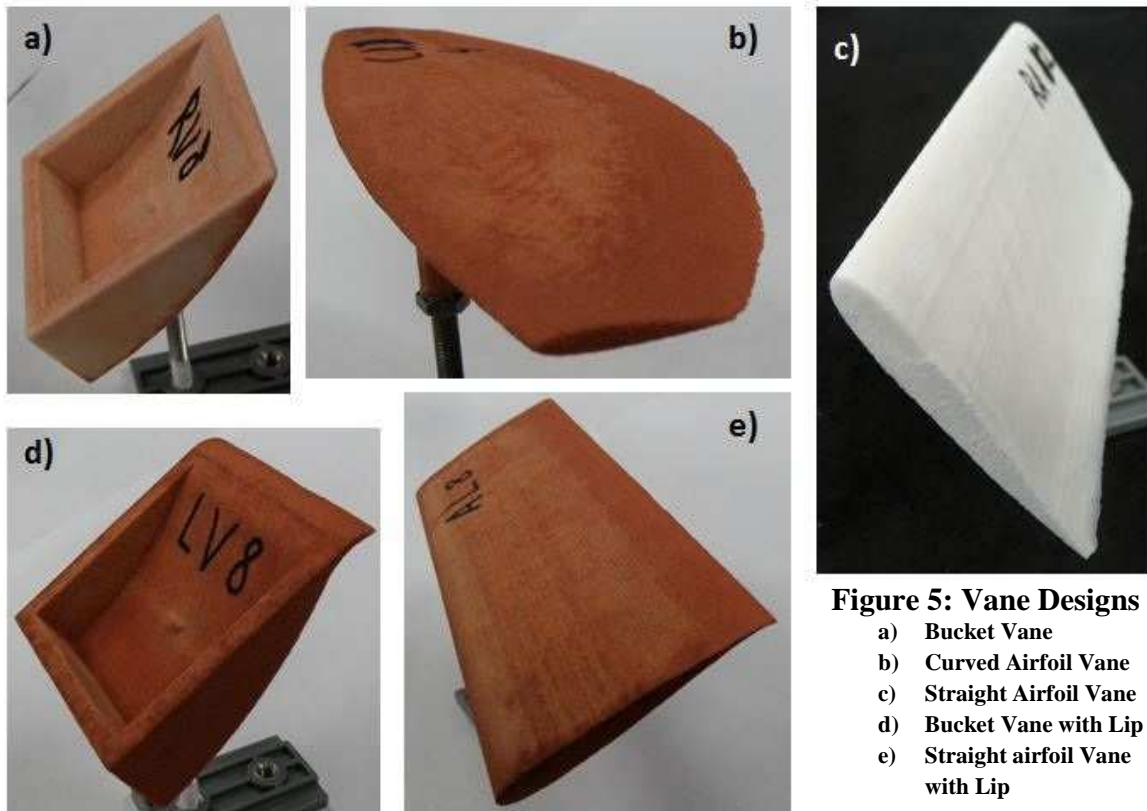


**Figure 5: Vane Designs**

- a) Bucket Vane
- b) Curved Airfoil Vane
- c) Straight Airfoil Vane
- d) Bucket Vane with Lip
- e) Straight airfoil Vane with Lip

The elliptical airfoil design was considered after finding research supporting the idea that an elliptical trailing edge is more efficient than an airfoil with a straight trailing edge [10]. The bucket vane idea was adopted from the design of a water wheel. Since that design is functional for water, it was assumed it would work for other fluids also, such as air. Eight possible positions on the rotor were selected (Figure 6) to be tested to provide a good estimate of the forces involved around the rotor. Thus, each of the five designs had eight different models corresponding to a certain position on the rotor. These actual designs were developed on PTC Pro/Engineer Wildfire 5.0 software. The models that were tested were created by exporting these files and fabricating them with a Zcorp ZPrinter® 310 Plus.

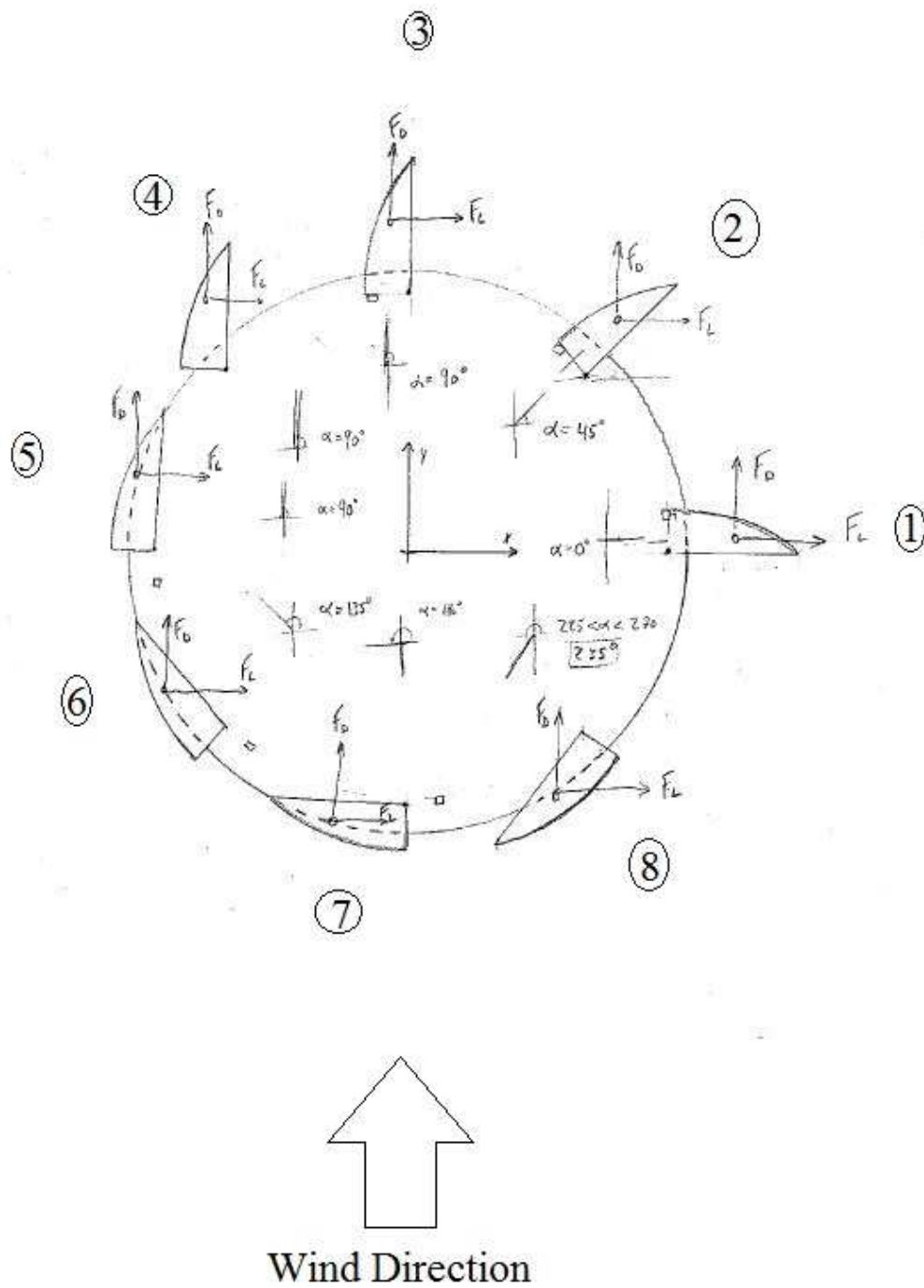


Figure 6: The eight selected vane positions on the rotor.

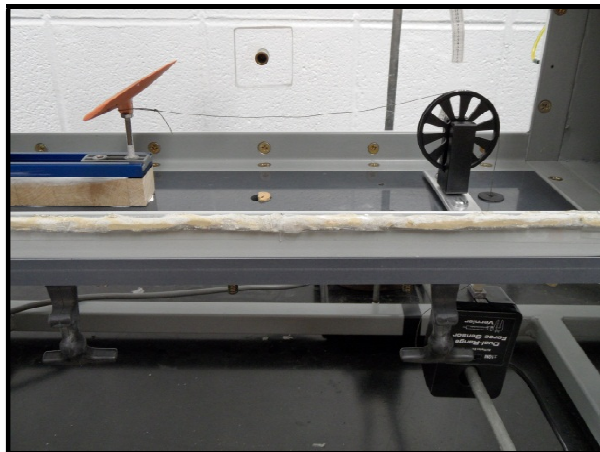
Once the models were printed, the base was first infiltrated with Gorilla Super Glue to give maximum strength to the junction between the vane and the mounting bolt. The model was then further infiltrated with Minwax Wood Finish to penetrate, and Minwax Polyurethane to seal.

These models were then tested using a GDJ inc. Model 360 Flotek Wind Tunnel (Figure 7) [13]. Two setups were required, one for the drag tests (Figure 8) and one for the lift tests (Figure 9). Each model was used for 12 tests on each of the test setups. These 30 second tests were a combination of four different wind speeds, with three repeats at each speed. The Vernier software, LoggerPro, was used to measure the forces involved for each setup.

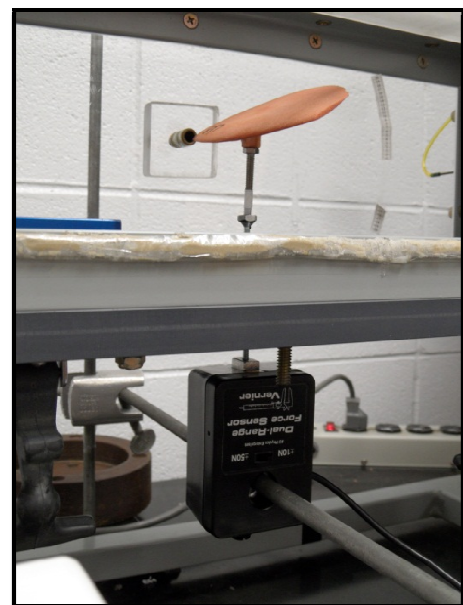
LoggerPro would yield an average force and a standard deviation that was recorded. The LoggerPro software required the recalibration of the force sensor every four to five vanes that were tested. The sensor was also zeroed after each run to eliminate the effects of hysteresis in the force sensor. The wind tunnel's air speed was measured using a manometer measuring in inches of water column, and then converted to Pascals.



**s used for the testing.**



**Setup**



**9: Lift Setup**

## Data Results and Calculations

The testing had some interesting developments. First, there seemed to be electrical interference on the force sensor that would scramble the readings on occasion. When this happened, the sensor was not precise enough to register good readings. The problem seemed to be fixed when the force sensor was isolated from the setup using electrical tape. Another observation noted was the presence of harmonic motion in the test setup for certain vanes. At certain wind speeds, the vane excited frequencies that showed up in the data. In many cases there was a sine curve that may be attributed to vortex shedding, which is a phenomenon that occurs frequently in fluids. Other possible causes were fan vibration and other structural vibrations. This variation was reduced in the results by using the average force measured.

The data was sorted into tables which used the two inputs, wind speed in inches of water column and the average force, to calculate Reynolds numbers and the coefficient of lift or drag. Equation 1 was used to calculate the Reynolds numbers for each trial to act as a measure of wind speed. Equation 2 was used to calculate the coefficients of drag and lift using the average force and its other equation components. In order to evaluate Reynolds number independence Excel was set up to plot the coefficient of drag data versus the Reynolds number as seen in Figures 10- 19.

When these data were collected for all the vane designs, they were compiled into a separate spreadsheet that did further analysis to relate the coefficients of lift and drag to the Net Torque on the rotor. Since  $Torque = Force \times Distance$ , the contribution of both the drag and lift forces estimated from the data is seen to have a measurable effect on the rotor's rotation. The distance was calculated using the rotor radius, and the distance along the vane to its center of mass. The center of mass is located at one fourth the chord length from the leading edge on the airfoil [9]. The i and j components of those lengths were then used to compute the vector cross-product with the force to determine the torque. The drag and lift forces are estimated using Equation 4 and Equation 5.

$$F_D = \frac{1}{2} \rho V^2 A C_D \quad \text{Equation 4}$$

$$F_L = \frac{1}{2} \rho V^2 A C_L \quad \text{Equation 5}$$

The net torque cannot be the value that is compared across the different vanes. The reason for this is the variation in the planform area of each of the different designs. One vane has a much larger area than another, so the amount of air pressing on it to create drag is larger as well. In order to place the vanes on the same playing field, the torques had to be normalized on a torques per unit area basis. This allows the vanes to be compared to each other. This was simply done using Equation 6.

$$Torque \text{ per Area} = \frac{Net \ Torque}{Planform \ Area} \quad \text{Equation 6}$$

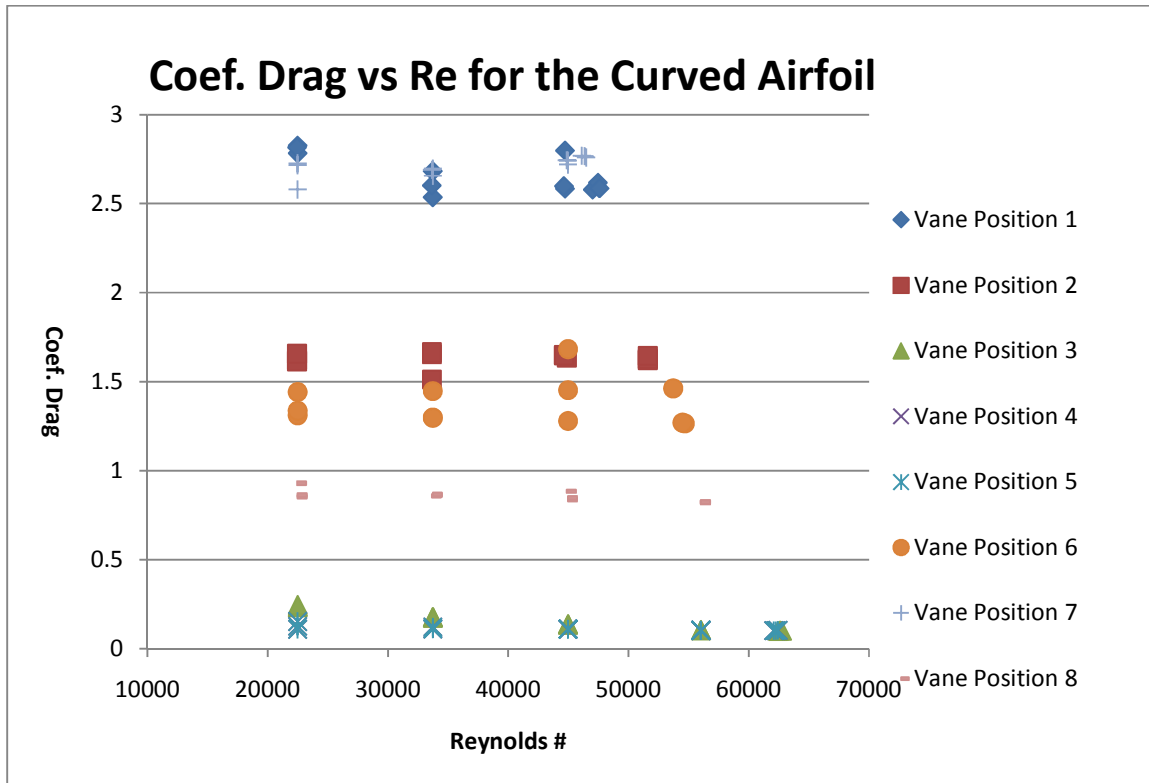


Figure 10: The graph of drag coefficient vs. Reynolds number of the Curved Airfoil.

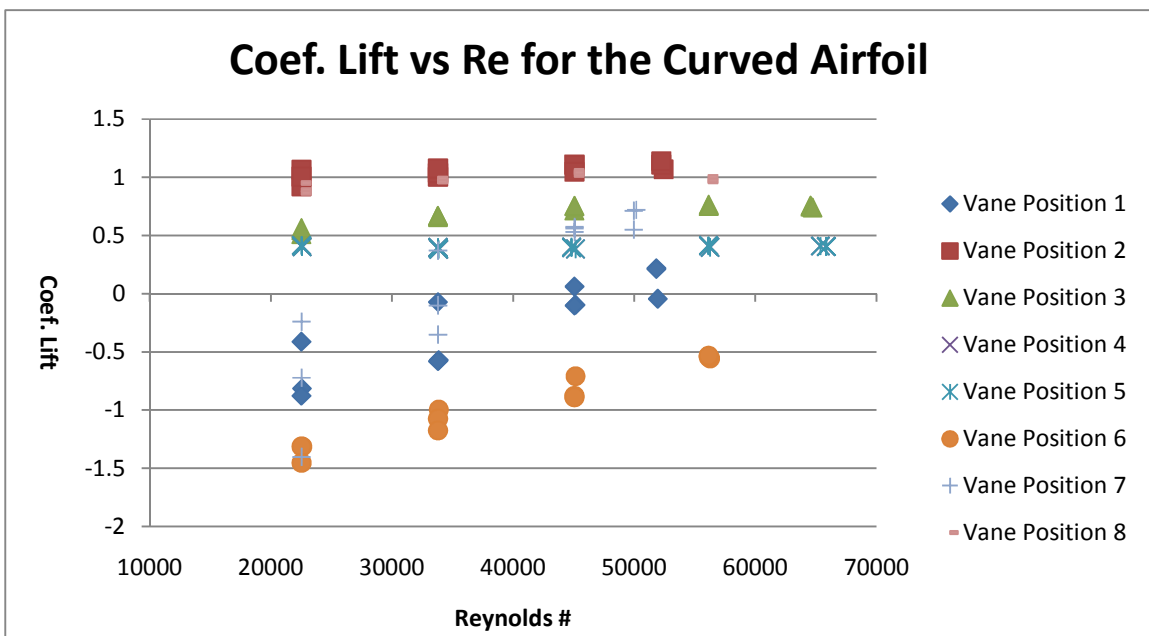
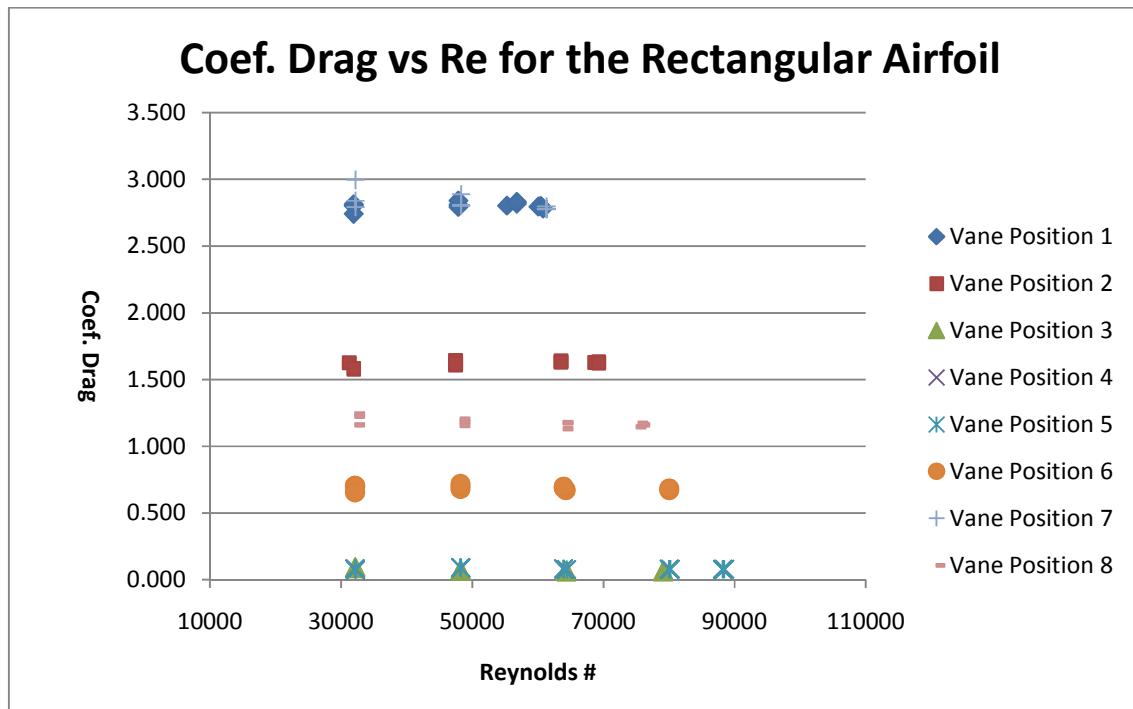
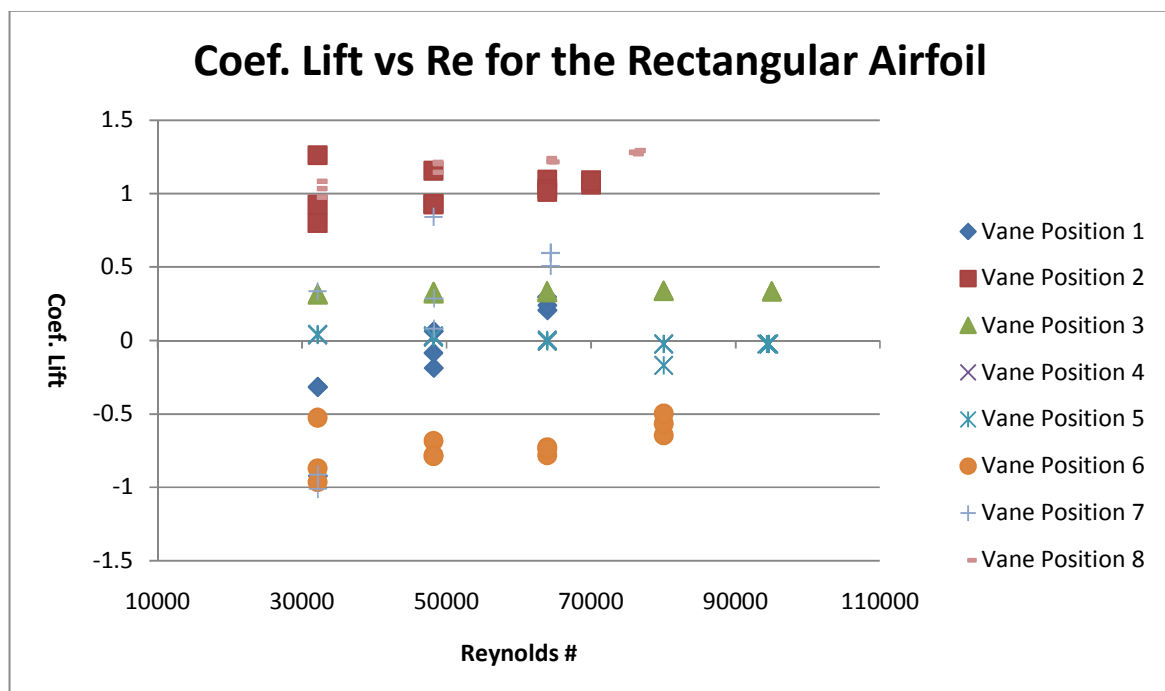


Figure 11: The graph of lift coefficient vs. Reynolds number of the Curved Airfoil.



**Figure 12:** The graph of drag coefficient vs. the Reynolds number of the Rectangular Airfoil.



**Figure 13:** The graph of lift coefficient vs. Reynolds number of the Rectangular Airfoil.



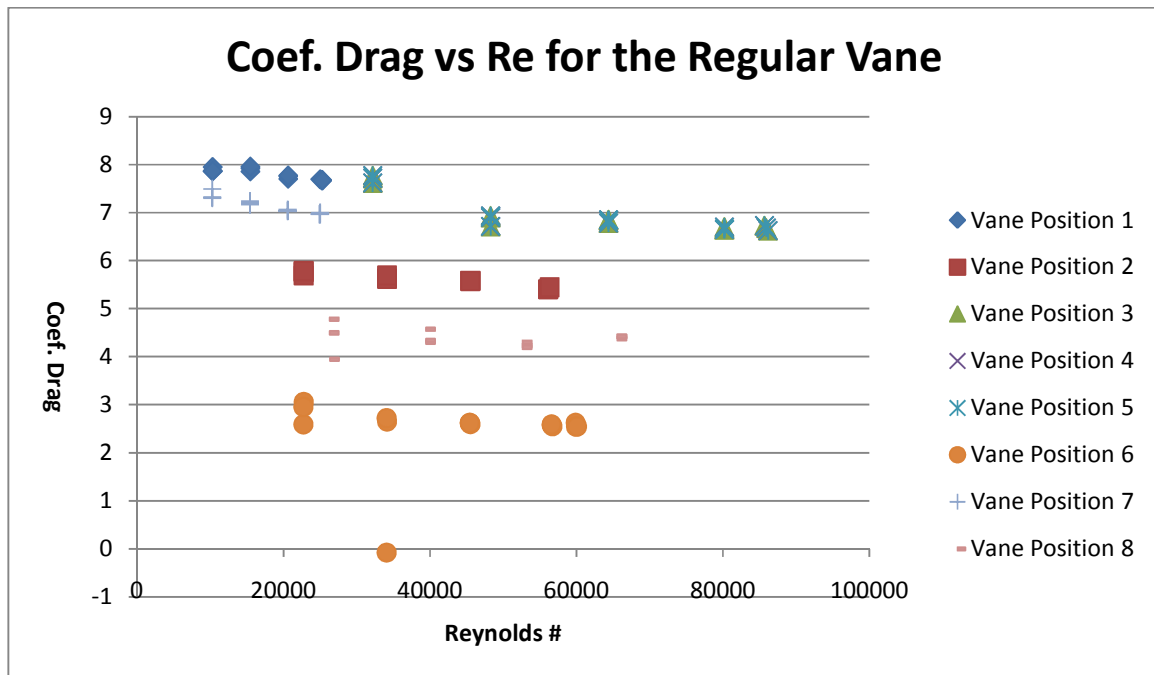


Figure 14: The graph of drag coefficient vs. Reynolds number of the Regular Vane.

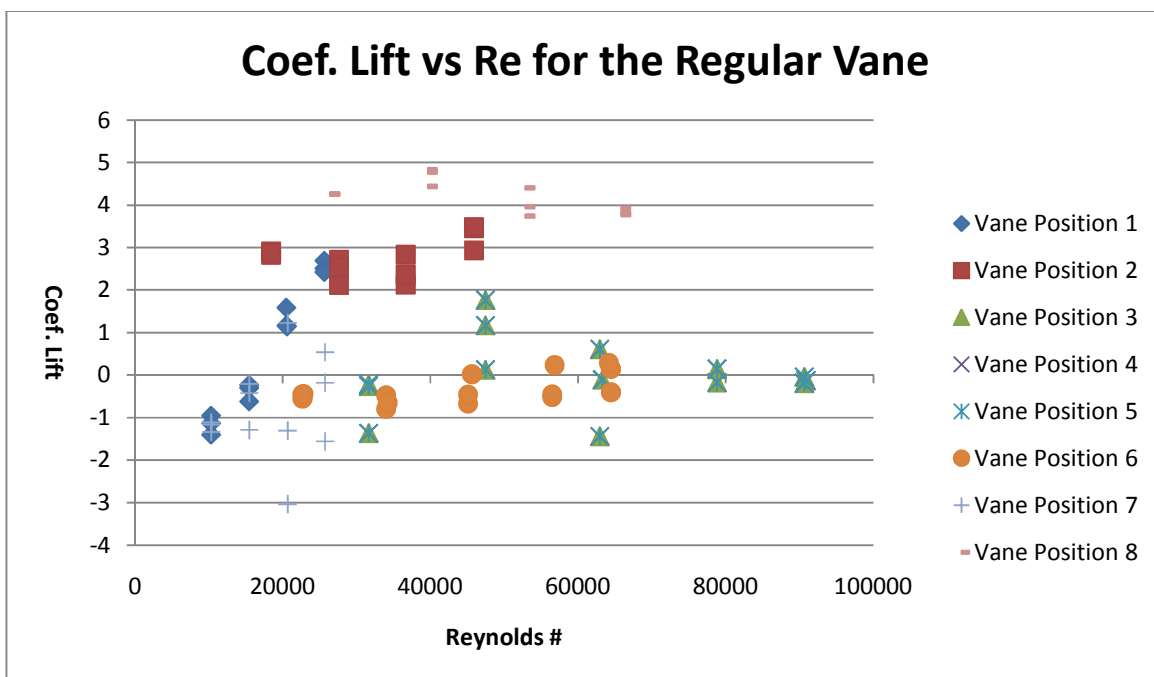


Figure 15: The graph of lift coefficient vs. Reynolds number of the Regular Vane.

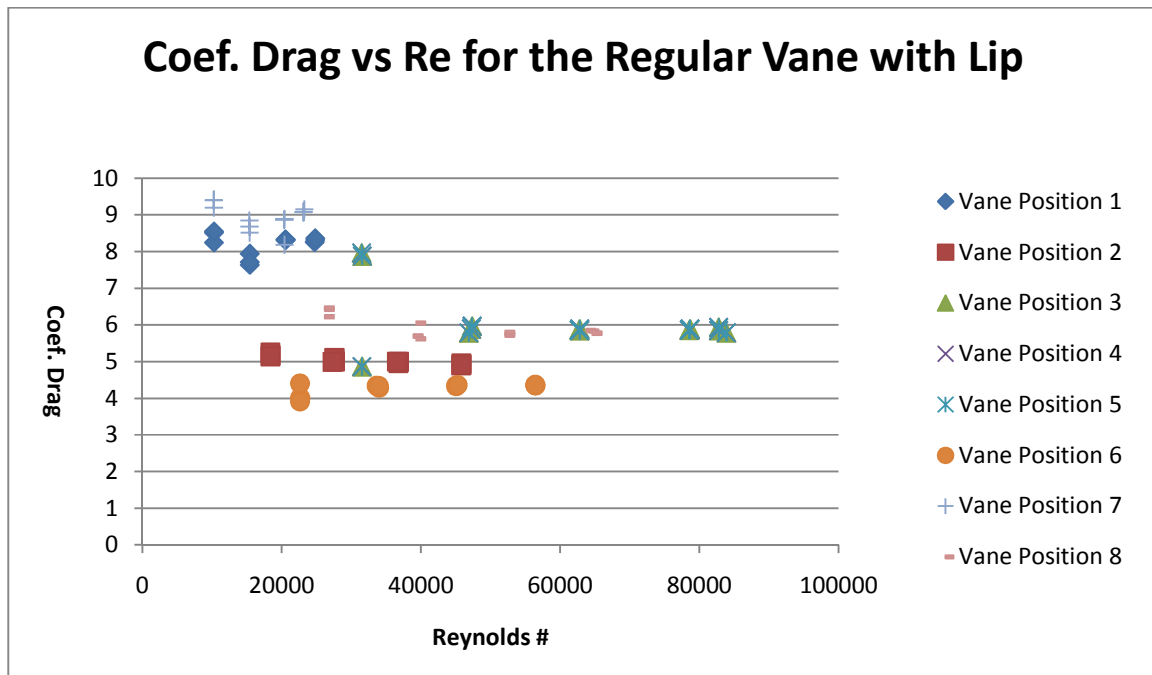


Figure 16: The graph of drag coefficient vs. Reynolds number of the Regular Vane with Lip.

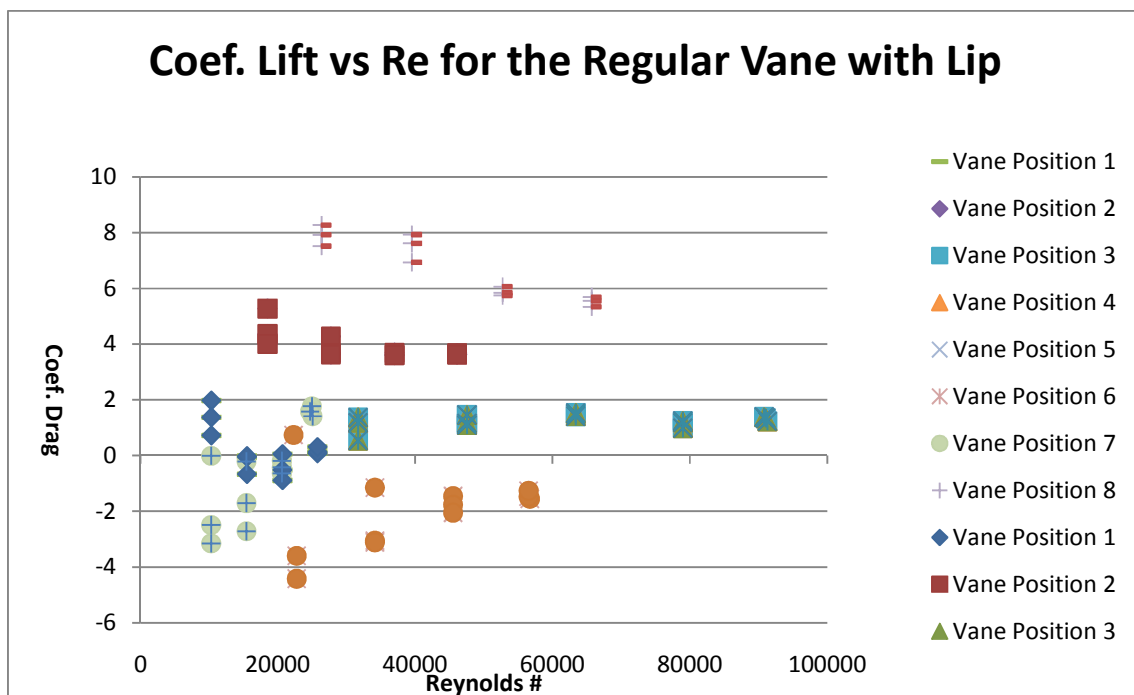


Figure 17: The graph of lift coefficient vs. Reynolds number of the Regular Vane with Lip.

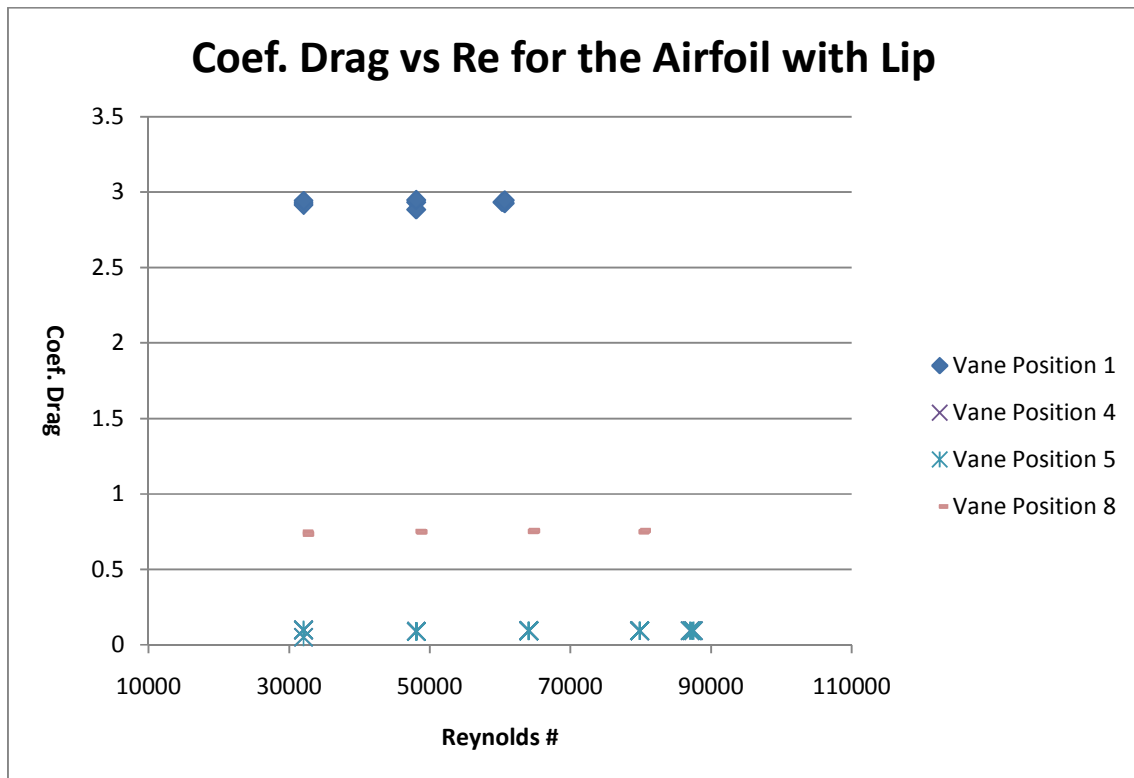


Figure 18: The graph of drag coefficient vs. Reynolds number of the Airfoil with Lip.

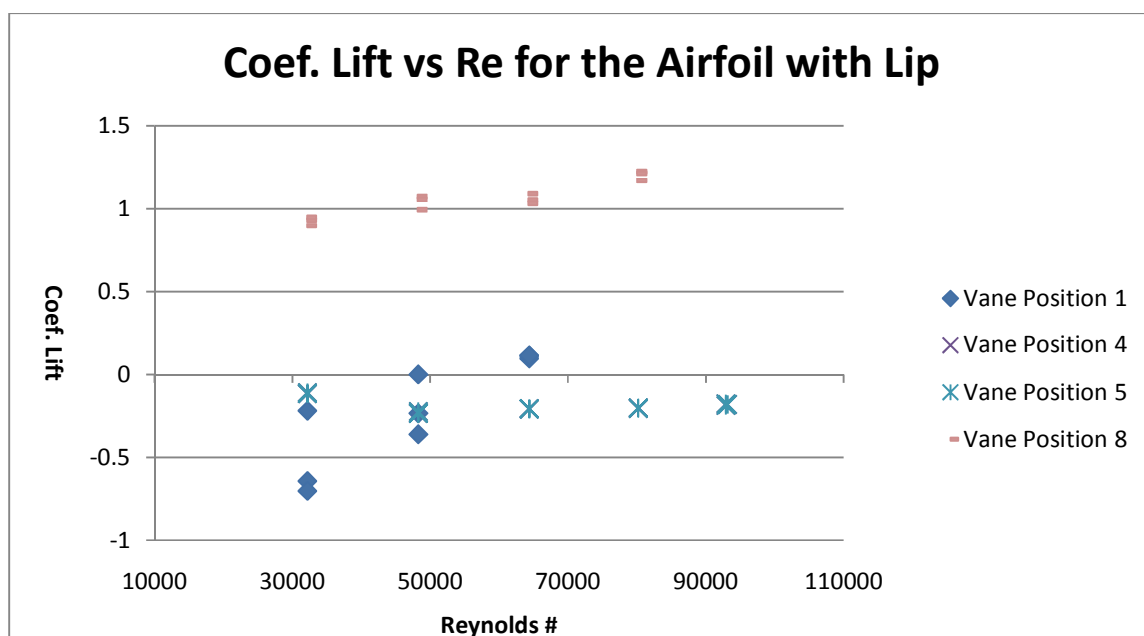


Figure 19: The graph of lift coefficient vs. Reynolds number of the Airfoil with Lip.

Using these data, the coefficients of drag and lift were estimated and the values outlined in Table 1 were selected. The drag coefficients were selected based on the Reynolds independence, but there is no clear relationship between Reynolds number and lift coefficient. For this research the assumption was made that the lift coefficient does not greatly change with Reynolds number. Therefore the values represented in Table 1 are rough averages of the range of data for each vane position and design.

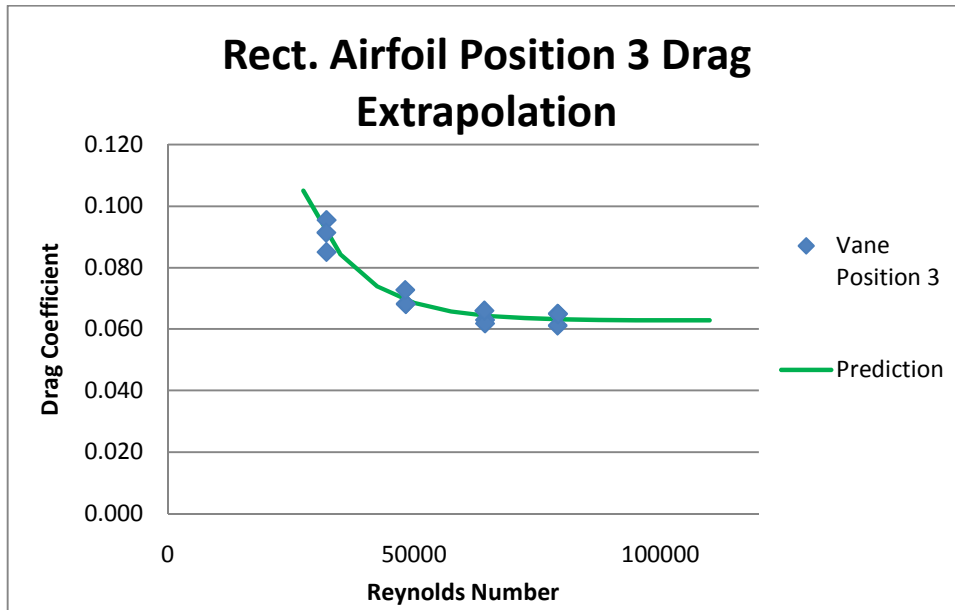
<b>Table 1: The coefficients of drag and lift obtained from the graphs.</b>										
	Rectangular Airfoil		Curved Airfoil		Regular Vane		Regular Vane w/ Lip		Airfoil with Lip	
<b>Vane Position</b>	$C_D$	$C_L$	$C_D$	$C_L$	$C_D$	$C_L$	$C_D$	$C_L$	$C_D$	$C_L$
<b>1</b>	5.61	-0.5	5.25	-0.5	7.8	1	8.2	-0.1	5.86	-0.5
<b>2</b>	3.25	2.2	3.27	2.1	5.6	2.5	4.9	3.7	n/a	n/a
<b>3</b>	0.12	0.66	0.15	1.3	6.7	0	5.8	1.25	n/a	n/a
<b>4</b>	0.16	0	0.225	0.8	6.7	0	5.8	1.25	0.18	0.1
<b>5</b>	0.16	0	0.225	0.8	6.7	0	5.8	1.25	0.18	0.1
<b>6</b>	1.36	-1.5	2.75	-2	2.6	-0.4	4.3	-1.5	n/a	n/a
<b>7</b>	5.6	1	5.45	0	7	-1	8.8	-0.5	n/a	n/a
<b>8</b>	2.3	2.3	1.7	1.9	4.3	4	5.8	6	1.55	1.5

Table 2 shows the values that were obtained using these calculations. These are estimates since they were calculated from coefficient information that had a certain amount of uncertainty. The error was calculated using the LoggerPro software. The stats function displayed the mean force as well as the standard deviation of the data. The uncertainty is given underneath the torque that was calculated using the wind tunnel test results. The error measurements were adapted by taking the standard deviation of the force and relating it to the torque. Figure 21 shows the torques per unit area of four first vane designs as displayed in Table 2.

<b>Table 2: Estimated Values for Torque.</b>		
	Torque [Nm]	Torque per Area [Nm/m <sup>2</sup> ]
Rectangular Airfoil	228 ± 14.1	1520 ± 94.3
Curved Airfoil	184 ± 2.9	1748 ± 27.7
Regular Vane	25 ± 2.4	1598 ± 153.4
LipVane	26 ± 2.8	1681 ± 184.4
Lip Airfoil	229 ± 11.25	1527 ± 75

## Analysis and Discussion

For these data to have statistical significance, the conditions of similarity must be met. The Reynolds number for the prototype situation with a wind speed of 25 m/s was calculated to be  $3.97 \times 10^5$ , but the fastest wind tunnel Re numbers were on the order of  $8 \times 10^4$ , which was not good enough for similarity. Since this was the case and there was limited time and budget, a water tunnel or a larger model and wind tunnel were not feasible. Thus, the next option available was extrapolating these data to the ranges of Reynolds numbers that were required for significance. Some of these data were reasonable enough that extrapolation would work, as seen in Figure 20, and resembles Reynolds number independence as seen in Figure 4.



**Figure 20: Data fitting the Reynolds number independence curve.**

The prediction curve is an equation especially suited for these data suggested by Dr. Schroeder to model the desired approach to Reynolds independence. It is an exponential curve fit with the equation:

$$C_D = C_1 * e^{-C_2 * Re} + C_3 \quad \text{Equation 7}$$

Where

- $C_D$  is the coefficient of drag
- $C_1$ ,  $C_2$  and  $C_3$  are coefficients computed by Excel
- $Re$  is the Reynolds number

This curve-fit line first has arbitrarily selected  $C_i$  values. Excel's solver program then optimizes the curve fit by choosing the  $C_i$  values to minimize the sum of the squares of the residuals. The residual is the difference at each data point between the data and prediction.

In some instances, the data were not consistent enough for this curve fit to be more than just a straight line. When this is the case, the distance that needs to be extrapolated is just too great. If the estimation is only slightly off the actual value, the error will be much greater after it has been extrapolated. These data were not as statistically helpful as was hoped. Therefore these data cannot be used to compare with data from other researchers since it does not meet the similarity constraints.

The purpose of these data was to help select the best vane of these five designs. The data, although not statistically conclusive, is still able to fulfill its purpose. Based on the how the drag coefficient vs. Reynolds number curve acts (seen in Figure 4), it is known that the data observed is higher than the independent drag coefficient [9]. Using this information the data can still be compared to indicate a "best" vane design.

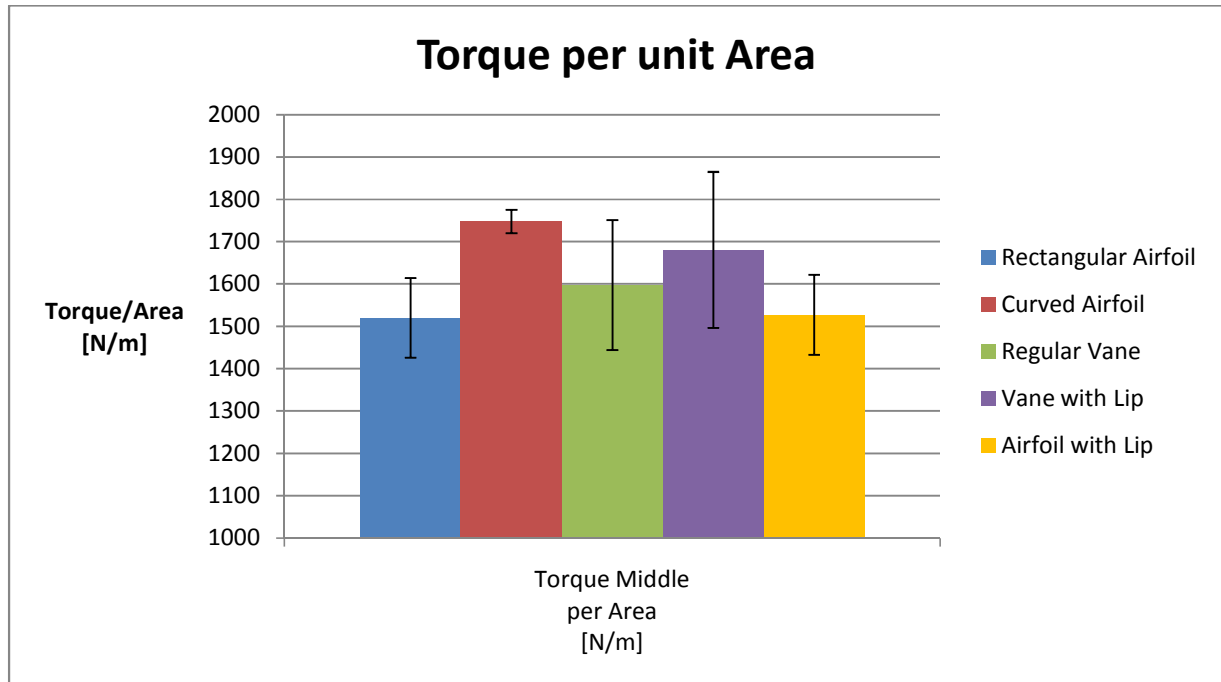


**Figure 21: Vane comparison**

The black error ranges shown in the top of each bar shows the variability in the data. The first things that are noticed are that the Curved Airfoil is the highest bar and has the smallest variation. All the other designs have a larger range that the actual value might fall in. The Rectangular Airfoil has the lowest torque values, and the Airfoil with Lip produces a net torque per unit area of 7 N/m greater than the Rectangular Airfoil. The data for the Regular Vane and the Vane with Lip both have variation zones that reach to or beyond the range for the Curved Airfoil. The problem is that the variation ranges are so large that they could perhaps yield the best torque, or very close to the worst torque possible. Thus, the Curved Airfoil should consistently perform within its relatively small range of torque values. Since all of the values in this torque range are higher than at least 50 percent of the torque ranges of the other vanes, the Curved Airfoil is determined to be the best choice for the rotor.

## Conclusion

The purpose of this study was to identify a functional vane that will lead to a net positive torque on the rotor of a VAWT. To accomplish this, five designs were selected and tested to see which would be the best choice to continue research with. All five designs achieved a positive net torque, and so all designs meet the minimum requirements for the rotor. Of the five designs the Curved Airfoil stands out due to its higher torque and considerably smaller variation zone. The higher torque may be attributed to it having less induced drag [10], and the smaller variation may be attributed to its ability to control vortex shedding that in turn reduced the sine curve vibrations. The coefficient of drag and coefficient of lift were plotted versus  $Re$  to establish grounds for  $Re$  independence, but the results were not conclusive.

As all the vane designs are reasonably similar in the torque they produce, it seems that the vane position may have more significance in the success of this VAWT design than the vane shape. Therefore, the mechanism that ensures the optimum vane position may be of greater importance than the vane

design. This project chose an airfoil as the main retraction mechanism; however, the performed tests did not gauge the potential of an airfoil closing mechanism. Further tests are encouraged to determine the exact capabilities of an airfoil closing mechanism.

Even though the results show a design that seems better suited to the needs of the turbine, these numerical results are not very accurate. Since all the tests were taken under similar conditions, these five vanes may be compared to one another. However, since Reynolds number independence was not met in the wind tunnel, the requirements for similitude were not met either. The resulting data were good enough to consider a best estimate for each vane and comparison, and for feasibility of the retractable vane concept, but will not satisfy the needs for coefficients of drag and lift comparisons. Other drag and lift data cannot reliably be compared to the results of this research.

## Relation to the Ultimate Goal

Now that the best vane design has been selected as the Curved Airfoil, the research may continue until a working prototype has been created. There are several areas that must be investigated before an efficient working prototype can be made. Further testing must be done to determine the capabilities of an airfoil retracting mechanism. Should this prove not to be a good method, another retracting mechanism must be identified and tested until a working system is identified. At that point a power study may be launched to determine or develop an efficient power converting process to change the kinetic energy into electrical energy. Also, there may be a number of vanes that optimize the power gleaned from the wind. Finally, a material needs to be selected so that the turbine may easily be fabricated in places with few resources. Now that the merit of this turbine design has been proven, it can continue on to become a reality.

## Cost Report

In the proposal, \$500 was set aside for Instrumentation, while \$400 was set aside for Materials and Fabrication. As it turns out, all the instrumentation already owned by the University was sufficient to get the data needed for this research. No new instrumentation was purchased. The materials needed to fabricate the models and the method of fabrication costs totaled \$124.64, well within the budget. The funds used are outlined in Table 3.

**Table 3: Cost Report**

Date	Reason	Price	Running Total
6/13/2011	Bolts	\$1.33	\$1.33
6/16/2011	Bolts	\$6.56	\$7.89
6/30/2011	Gorilla Super Glue	\$5.97	\$13.86
7/5/2011	MinWax Stain	\$8.99	\$22.85
7/7/2011	Polyurethane and bolts	\$14.79	\$37.64
7/25/2011	Printing Costs	\$87.00	\$124.64
<b>Total</b>			<b>\$124.64</b>

## Research Impact

This research has been a great learning experience for me as I have picked up many skills that will help me in my life. I have never excelled in literature searches, and finding sources. During the last 10 weeks I have learned tricks and been given advice on how to use my literature search time wisely. For example, when I am researching to learn about various ways to set up for testing, I will contact the Technical Support of the company that manufactures the instrumentation I plan to use and see if they have any literature to offer relating to my studies. This skill will greatly benefit me as I plan to attend Graduate School. I have developed the habit of journaling what I am working on and what my thoughts are about it. This has proved itself a great help when I was preparing this report. I was able to look back in my notes and relate some observations and feelings about the project I had forgotten about. I have learned how to be productive and prepared in meetings. My meetings with Dr. Schroeder have prepared me to present the status of a project, and how to open discussion about a certain issue. This will increase my value as an Engineer.

I have also learned skills in Microsoft Word, Excel, and OneNote that will allow me to organize my life and schooling more efficiently in the future. I have also learned skills in those programs that will help me in my professional life as an Engineer.

I have learned to use the University's wind tunnel and 3D printer, and I am currently the only student attending Olivet that knows how to use and take care of that equipment. This will allow me to share that knowledge with other students as they work on various projects of their own. This has allowed me to become a help and an asset to the Engineering Department.

## Special Thanks

I wanted to take a moment and a section to express my appreciation to the people who have helped me. First, I want to say thank you to the Pence Boyce program and their supporters for being able and willing to fund my project. I have learned skills through this work that I would not have obtained elsewhere. I thank you for giving me this great opportunity. Next, thanks to the members of the Pence Boyce committee that selected my project to be funded. I am so glad you gave me this chance. I also want to thank Dr. Schroeder for spending the time and going the extra mile to help me with what I needed. You have taught me more in these 10 weeks than in any class about research, school and life. Rick Shelton has been a great help and enthusiastic observer with the creation and fabrication of the test setup and models. Thanks Rick! I also want to express my appreciation to the rest of the Engineering department faculty. They have all helped me from time to time, and supported me in this research as well as in my schooling. Thanks also to anyone I forgot to mention.



## References

- [1] Pramod Jain, *Wind Energy Engineering*. New York: McGraw-Hill, 2011.
- [2] Thomas Ackermann, *Wind Power in Power Systems*. Hoboken, NJ: John Wiley & Sons, Ltd, 2005.
- [3] (2010, June) U.S. Department of Energy, Energy Efficiency & Renewable Energy. [Online].  
[http://www1.eere.energy.gov/windandhydro/wind\\_technologies.html](http://www1.eere.energy.gov/windandhydro/wind_technologies.html)
- [4] A. J. Alexander and B. P. Holownia, "Wind Tunnel Tests on a Savonius Rotor," *Journal of Industrial Aerodynamics*, pp. 343-351, 1978.
- [5] Ben F. Blackwell, Robert E. Sheldahl, and Louis V. Feltz, "Wind Tunnel Performance Data for Two- and Three-Bucket Savonius Rotors," Albuquerque, NM, Government Report 1977.
- [6] Kunio Irabu and Jitendro Nath Roy, "Study of direct force measurement and characteristics on blades of Savonius rotor at static state," *Experimental Thermal and Fluid Science*, pp. 653-659, 2011.
- [7] U. K. Saha, S. Thotla, and D. Maity, "Optimum design configuration of Savonius rotor through wind tunnel experiments," *Journal of Wind Engineering and Industrial Aerodynamics*, pp. 1359-1375 , 2008.
- [8] J. F. Manwell, J. G. McGowan, and A. L. Rogers, *Wind Energy Explained*. Hoboken, NJ: John Wiley & Sons, Ltd, 2002.
- [9] John M. Cimbala and Yunus A. Cengel, *Essentials of Fluid Mechanics: Fundamentals and Applications*. Boston: McGraw-Hill Higher Education, 2008.
- [10] David F. Anderson and Scott Everhardt, *Understanding Flight*. New York: McGraw-Hill, 2010.
- [11] Frank M. White, *Fluid Mechanics*, 7th ed. New York: McGraw-Hill, 2008.
- [12] Jens Trapp and Robert Zores. (2009, February) NACA 4 Digits Series Profile Generator. [Online].  
<http://www.ppart.de/aerodynamics/profiles/NACA4.html>
- [13] GDJ. (2008) GDJ INC. [Online]. <http://www.gdjinc.com/windtunnels/wind2.html>

## Appendix



**Figure 22: Low Friction Track used for the Drag Tests.**

### Wind Tunnel Setup (Drag)

The low friction track (Figure 22) was mounted on the wind tunnel test area bottom section. The pulley was then mounted on the floor of the test area lined up with the hole for the string. Next, the bolt part of the vane was threaded into the low friction slider. It is important that the pulley and the airfoil are at the same height. If not, the angle would introduce avoidable error. Adjustments will be made using the angle it is off the horizontal in order to get good results. The distance between the pulley and the low friction track was as far as reasonably possible to reduce that angle off the horizontal. Also, the farther the pulley is, the less effect it will have on the wind and how it moves around the airfoil. The mounted airfoil was then set on the front of the track (closer to the pulley). After the force sensor was calibrated, it was mounted underneath the hole in the wind tunnel floor as seen in the Figure 23. A line was attached to the front of the airfoil and around the pulley to the

Dual Force Sensor. The line was taut and horizontal to minimize error. The software LoggerPro and Dual-Range Force Sensor from AU Physics Enterprises and Vernier was used to measure the forces experienced by the models during testing.

### Configuring LoggerPro

In order to get LoggerPro ready to collect the data, the sensor must be calibrated. The data collection file for dual force sensors is located under Experiments/Probes & Sensors/Force Sensors/Dual Range Force Sensors. The file required for these tests is the 10N Dual Range.cmbl. To calibrate the force sensor, the sensor was mounted so it could measure weight as seen in Figure 24. In LoggerPro, the calibrate function is located in the Experiment tab >> Calibrate >> Dual Range Force. In the Sensor Settings the



**Figure 23: Force sensor location for drag tests.**

calibrate tab was selected and the Calibrate Now button pressed. After making sure there was nothing on the force sensor, "0" was inputted into Reading 1 and the Keep button selected. For the second value a 50 gram weight was placed on the force sensor and after entering the value 0.49 in the field for Reading 2 the Keep button was pressed again. That is how the sensor was calibrated.

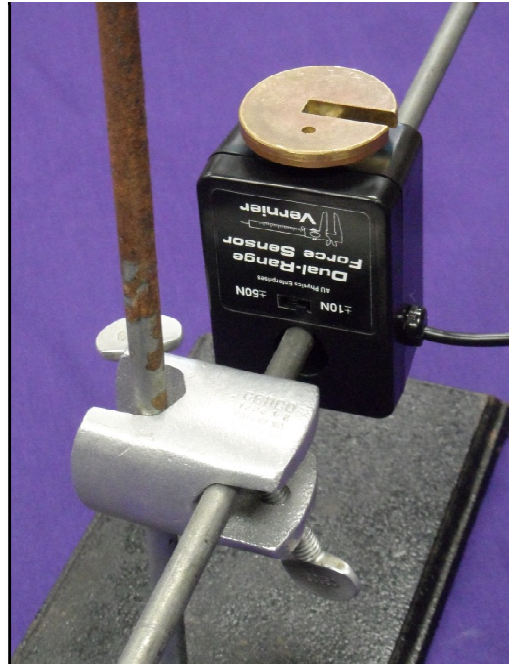


**Figure 24: Setup for Sensor calibration.**

### **Wind Tunnel Setup (Lift)**

After all the apparatus from the drag measurement setup was removed, the Force Sensor was moved to be right below the hole in the center of the floor board (Figure 25). The airfoil was then fixed threaded straight bolt and mounted through the center hole in the floor board to the dual force sensor.



**Figure 25: Force Sensor location for Lift tests.**

### Testing Procedure

The first thing to do is to set the collection time to 30 seconds. This was done using the commands in the collections menu which is accessed by clicking the data collections button. The sensor was zeroed by selecting the Zero button on the toolbar. This was done before every test. The temperature was then measured in Celsius, using a glass thermometer, and recorded in the data table corresponding to the vane type in the Temp [C] column. When turning on the wind tunnel, the controls were first set to zero to avoid an impulse response from the model. While watching the Manometer, the speed was increased until the correct pressure value was reached. The given pressure from the manometer was then recorded in the "Measured Height" column. At this point the LoggerPro software was activated by pressing the "Collect" button. Each trial runs for 30 seconds to provide a consistent average force. The tunnel was then turned off, and the speed control set to zero. To get the data from the LoggerPro software, a trend line of the data was created by pressing the "Statistics" button in the toolbar. After the mean force value was documented in the data table, the file was saved and a new file opened in LoggerPro. Steps 2-11 were repeated for each of the preselected velocities given in the data table. This was then repeated for each of the vanes whose drag and lift forces were measured.